X-RAY AMORPHOUS AND POORLY CRYSTALLINE FE-CONTAINING PHASES IN TERRESTRIAL FIELD ENVIRONMENTS AND IMPLICATIONS FOR MATERIALS DETECTED ON MARS. A. D.
Feldman[1], E. M. Hausrath[2], O. Tschauner[2], P. Burnley[2], A. Lanzirotti[3], E. B. Rampe[4], T. Peretyazhko[4], W. Calvin[5], B. Azua[2], C. T. Adcock[2], [1]University of Nevada, Las Vegas (feldma2@unlv.nevada.edu), [2]University of Nevada, Las Vegas, [3]University of Chicago, [4]NASA Johnson Space Center, [5]University of Nevada, Reno

Introduction: Recent analyses of X-ray diffraction (XRD) data from the CheMin instrument using the FULLPAT program have documented the presence of X-ray amorphous materials at multiple sites within Gale Crater, Mars [1–4]. These materials are believed to be to be iron-rich based on chemical data, and at least some of them are believed to be weathering products based on volatile contents [1,4-6]. However, the characteristics of these proposed Fe-rich weathering products remain poorly understood. To better understand these X-ray amorphous materials on Mars, we are 1) examining weathering products formed on Fe-rich parent material in terrestrial soils across a range of climatic conditions, and 2) performing burial experiments of Fe- and Mg- rich olivine in these soils. We describe each of these approaches below.

Examination of Weathering Products To evaluate weathering products formed on Fe-rich parent materials across a range of climates, we investigated soils formed on ultramafic parent materials in the Tablelands of Newfoundland, Canada (subarctic), Pickhandle Gulch in Nevada (cold desert), and the Klamath Mountains of California (mediterranean). The Tablelands and Klamath Mountains possess sites that were deglaciated 12,000 to 15,000 years before present [7,8]. The Klamath Mountains also contain older soils that were not glaciated for comparison. Previous work has identified X-ray amorphous material in the toe-slope of a soil catena in the Klamath Mountains [9] and we therefore selected toeslope locations for sampling.

Emplacement of Fe- and Mg-rich Olivine Samples Olivine weathering is proposed as a contributor to the formation of Fe- and Mg- rich weathering products on Mars [10]. Olivine has also been proposed as an indicator of aqueous alteration on Mars due to its rapid rate of dissolution [11–13]. To test variations in incipient dissolution of the Fe- and Mg- rich end members of the olivine solid solution series, forsterite (Mg_2SiO_4) and fayalite (Fe_2SiO_4), we buried olivine within soils developing on the Tablelands, and will bury olivine within soils developing at Pickhandle Gulch. We will collect burial samples following one to two years and will examine etch pit formation, surface leaching, and formation of secondary products.

Methods:

Sample Collection Four soil pits were excavated at each of the Klamath Mountains and Tablelands field sites. Within the Klamath Mountains, we selected two sampling sites within the Trinity Ultramafic Body (TUB), Eunice Bluffs (EB) and Deadfall Lake (DfL), and two within the Rattlesnake Creek Terrane (RCT), String Bean Creek (SBC) and Round Mountain (RM), to ascertain differences between areas of greater (TUB) and lesser (RC) serpentinization [14]. Soil pit excavation at Klamath Mountain field sites continued to the point of bedrock contact for the younger relatively undeveloped soils of the TUB and into the C horizon for the older more developed soils of the RCT. On the Tablelands soil pits excavation continued either to the bedrock contact or slightly below the local water table. Following field description of soil horizonation, we sampled from the A horizon and at 10 cm increments below the A horizon, with samples collected from the B and C soil horizons when present.

Preparation of Fe- and Mg- Rich Olivine Samples for Emplacement Fayalite samples were prepared by annealing synthetic fayalite powder within a Griggs apparatus [15] at 900°C. The powder was prepared by mixing 28.0948 g of 99.5% pure Fe- powder, 80.3157 g of 99.8% pure Fe_2O_3, and 45.3349 g 99.5% pure SiO_2 powder, sealing the powder under vacuum and flushing with Ar gas, and firing the powder mixture for 3 days at 950°C. Cut fayalite samples were embedded within epoxy disks, and where nickel jacketing from the Griggs press was present, a coat of acrylic enamel was applied to prevent nickel exposure. Forsterite samples were cut from a 7 cm diameter column of 97% Forsterite with 3% co-existing Enstatite ($MgSiO_3$) prepared by hot pressing at 1400°C and 100 MPa (forsterite preparation is described in [16]). All fayalite and forsterite samples were polished to a 0.25-μm polish level after cutting.

Emplacement of Samples We buried olivine disks at all four sites within the Tablelands and will bury olivine disks at Pickhandle Gulch in early 2019. Polished forsterite and fayalite disks were emplaced within 250 mL LDPE bottles with holes drilled in them after [17]. After filling bottles halfway with soil, polished olivine disks were inserted into the bottles, the remainder of the bottles filled with soil, and the

bottles placed into the excavated soil pits. Samples were buried within B horizons if identified, and within the center of the soil column if no B horizon was observed. At one Tablelands sample site, burial sample emplacement was located below the water line to provide a comparison with samples buried above the water line at all other Tablelands sites. Two control samples of fayalite and forsterite are stored within the Hausrath soil lab for the duration of the experiment.

Sample Analysis Klamath Mountain soils have been characterized for standard soil properties including Munsell color, clay film accumulation, ped structure, gravel content, texture, consistency, and horizon boundaries. Subsequently, the clay size fraction was extracted following the methods of [18]. The clay size fraction was analyzed via the following: a Proto-AXD Bragg-Bentano type powder diffractometer using a Cu K-alpha tube (1.541 Å wavelength) with a Dectris hybrid pixel array detector and Soller slits, SEM/EDS, and synchrotron techniques including µXRD, µXRF, XANES, and EXAFS on beamline 13-IDE at Advanced Photon Source. We collected XANES scans at the Fe K-edge (7110.75 eV) for the clay-size fraction from the B horizon for each sample, fit the spectra with 1-3 Gaussian functions, and identified the centroid position utilizing the program Larch (e.g. Figure 1).

Results and Discussion: µXRF mapping indicates the presence of iron in most of the clay size fraction of the Klamath Mountains soils. Powder and synchrotron XRD analyses indicate the presence of lizardite, talc, tremolite, smectite, illite, and iron oxyhydroxides including goethite and ferrihydrite. Reddening of the B horizons within the older non-glaciated soils also suggests accumulation of iron oxyhydroxides. Smectite present in the older soils appears more crystalline as indicated by sharper XRD peaks in the powder diffraction patterns than the smectite present in the younger soils. The presence of X-ray amorphous materials is inferred from an elevated background signal. µXRD measurements lack a similar elevated background signal, suggesting that much of the material that is identified within the X-ray amorphous component of the powder diffraction data is nano-crystalline rather than truly amorphous. Centroid positions identified in Fe-XANES spectra, which have previously been shown to reflect Fe-oxidation state [19,20], indicate that soils from the Klamath Mountains possess a mixture of Fe(II) and Fe(III) (Figure 2). The higher proportion of Fe(II) in the Round Mountain and String Bean Creek soils is likely a result of less serpentinized parent material [14].
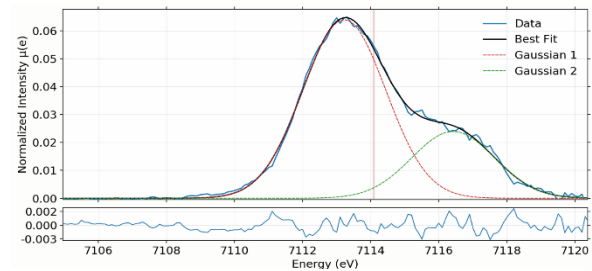

Figure 1: XANES pattern for a String Bean Creek soil sample, fit by 2 Gaussian functions, bottom section shows the residual after the best fit. Centroid position is denoted by the vertical red line.
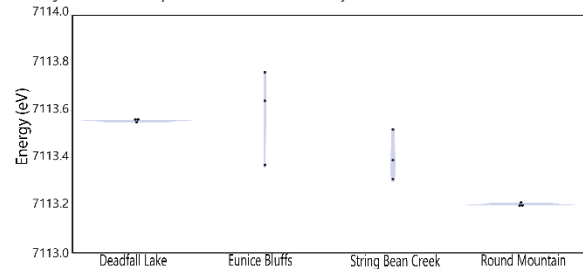

Figure 2: Klamath Mountain sample centroid positions

References: [1] Achilles, C. N., et al (2017) *GRP* 122, 2344-2361. [2] Morris R. V. et al. (2016) *NASA Working Doc.* [3] Yen, A. S. et al. (2017) *EPSL* 471, 186-198. [4] Rampe, E. B. et al. *EPSL* 471, 172-185 [5] Ehlmann B. L. et al. (2017) *GRP.* 122, 2510-2543. [6] Sutter B. et al. (2017). *GRP.* 122. 2574-2609. [7] Osborn G. et al. (2007) *Can. J. Earth Sci.* 44, 819-834 [8] Daniels M. L. & Whitlock C. (2005). *The Holocene.* 15, 1062-1071. [9] Istok J. D. & Harward M. E. (1982) *Soil Sci. Soc. Am. J.* 46, 1106-1108 [10] Bristow T. F. et al. (2015) *Am. Min.* 100, 824-836. [11] Ody A. et al. (2013) *GRP.* 118, 234-262. [12] Olsen A. A. and Rimstidt, J. D. *Am. Min.* 92, 598-602. [13] Stopar J. D. et al. (2003) *Sixth Int. Conf. on Mars.* [14] Alexander E. B. (2004) *Int. Geo. Rev.* 46, 754-764 [15] Griggs, D. T. & Kennedy G. C. (1956) *Am. J. Sci.* 254, 722-735. [16] G Xia (2013) *Diss. UC-Riverside.* [17] Nugent M. A. et al. (1998) *Nature.* 395, 588-591. [18] Edwards A. P. & Bremner J. M. (1967) *J. Soil Sci.* 18, 47-63 [19] Wilke et al. (2001) *Am. Min.* 86, 714-730 [20] Debret B. et al (2014) *EPSL.* 400, 206-218